# Supplementary material for "Toward speed-of-sound anisotropy quantification in muscle with pulse-echo ultrasound"

Naiara Korta Martiartu, Saulė Simutė, Michael Jaeger, Thomas Frauenfelder, and Marga B. Rominger

## I. Content

This supplementary material shows the detailed derivation of equations summarized in the main manuscript and figures clarifying the results shown in Figs. 4 and 9b.

## II. Traveltimes in elliptically anisotropic media

In a medium with elliptical anisotropy, the group velocity of longitudinal waves $v(\theta)$ in an arbitrary propagation direction $\theta$ satisfies

$$\frac{v^2(\theta)}{v_1^2}\sin^2(\theta-\varphi)+\frac{v^2(\theta)}{v_2^2}\cos^2(\theta-\varphi)=1, \tag{1}$$

where $v_1$ and $v_2$ are the longitudinal-wave velocities along and across the anisotropy symmetry axis, respectively, and the angle $\varphi$ indicates the orientation of this axis with respect to our reference system [see Fig. 1(a) in the main manuscript]. Equivalently, we can rewrite this equation as

$$\frac{1}{v^2(\theta)}=\frac{1}{v_1^2}\sin^2(\theta-\varphi)+\frac{1}{v_2^2}\cos^2(\theta-\varphi) \tag{2}$$

to explicitly define $v(\theta)$.

In homogeneous media, the traveltime of longitudinal waves propagating between arbitrary locations $\mathbf{x}_\mathrm{A}$ and $\mathbf{x}_\mathrm{B}$ is generally given by

$$t_\mathrm{AB}=\frac{||\mathbf{x}_\mathrm{B}-\mathbf{x}_\mathrm{A}||}{v(\theta)}, \tag{3}$$

where $||\cdot||$ refers to the Euclidean norm, and $\theta$ is the angular position of $\mathbf{x}_\mathrm{B}$ with respect our the coordinate system, with its origin at $\mathbf{x}_\mathrm{A}$ [see Fig. 1(a) in the main manuscript].

After taking the square of (3) and replacing $v(\theta)$ with the definition given in (2), we obtain

$$t_\mathrm{AB}^2=\frac{||\mathbf{x}_\mathrm{B}-\mathbf{x}_\mathrm{A}||^2}{v_1^2}\sin^2(\theta-\varphi)+\frac{||\mathbf{x}_\mathrm{B}-\mathbf{x}_\mathrm{A}||^2}{v_2^2}\cos^2(\theta-\varphi). \tag{4}$$

This equation can be simplified by applying standard trigonometric identities and using the geometric relations $||\mathbf{x}_\mathrm{B}-\mathbf{x}_\mathrm{A}||\sin\theta = x_{1,\mathrm{B}}-x_{1,\mathrm{A}}$ and $||\mathbf{x}_\mathrm{B}-\mathbf{x}_\mathrm{B}||\cos\theta = x_{2,\mathrm{B}}-x_{2,\mathrm{A}}$. Finally, we can express the traveltime $t_\mathrm{AB}$ as

$$t_\mathrm{AB}^2=\frac{1}{v_1^2}\left[(x_{1,\mathrm{B}}-x_{1,\mathrm{A}})\cos\varphi-(x_{2,\mathrm{B}}-x_{2,\mathrm{A}})\sin\varphi\right]^2+\frac{1}{v_2^2}\left[(x_{1,\mathrm{B}}-x_{1,\mathrm{A}})\sin\varphi+(x_{2,\mathrm{B}}-x_{2,\mathrm{A}})\cos\varphi\right]^2. \tag{5}$$

## III. Reflector-based experimental setup: derivation of the reflection point

Let us consider a reflector-based experimental setup with the reflector parallel to the ultrasound probe [see Fig. 1(b) in the main manuscript]. We can use Fermat's principle to analytically derive the first-arrival reflection traveltime $t_\mathrm{SR}$ of waves propagating from a source at $\mathbf{x}_\mathrm{S}$ to a receiver at $\mathbf{x}_\mathrm{R}$ as

$$\min_{\mathbf{x}_\mathrm{P}\in\mathcal{D}} t_\mathrm{SR}(\mathbf{x}_\mathrm{P}), \quad \text{where} \quad t_\mathrm{SR}(\mathbf{x}_\mathrm{P})=t_\mathrm{SP}(\mathbf{x}_\mathrm{P})+t_\mathrm{PR}(\mathbf{x}_\mathrm{P}). \tag{6}$$

Here, $\mathcal{D}$ refers to the set of points $\mathbf{x}_\mathrm{P}$ at the reflector-tissue interface [see Fig. 1(b) in the main manuscript], and traveltimes of each path are computed using (5).

Naiara Korta Martiartu was with the Zurich Ultrasound Research and Translation (ZURT) group, Institute of Diagnostic and Interventional Radiology, University Hospital Zürich, Zürich CH-8091, Switzerland, and is now with the Institute of Applied Physics, University of Bern CH-3012, Switzerland (e-mail: naiara.korta@unibe.ch).

Saulė Simutė was with the Department of Earth Sciences, ETH Zurich, Zurich CH-8092, Switzerland.

Michael Jaeger is with the Institute of Applied Physics, University of Bern CH-3012, Switzerland.

Thomas Frauenfelder, and Marga B. Rominger are with the ZURT group, Institute of Diagnostic and Interventional Radiology, University Hospital Zürich, Zürich CH-8091, Switzerland.

In a first step, we compute the location of the reflection point $\mathbf{x}_{\text{P}}^{\text{min}}$ satisfying (6). We assume that this point is shifted from the source-receiver mid-point position by the same constant $\delta$ for every source-receiver combination, i.e., $\mathbf{x}_{\text{P}}^{\text{min}} = ((x_{1,\text{S}} + x_{1,\text{R}})/2 + \delta, L)$. To find the value of $\delta$, we consider, for simplicity, the zero-offset case in which $\mathbf{x}_{\text{S}} = \mathbf{x}_{\text{R}}$, and we solve (6) using

$$\left.\frac{dt_{\text{SR}}}{dx_{1,\text{P}}}\right|_{\mathbf{x}_{\text{P}}=\mathbf{x}_{\text{P}}^{\text{min}}} = 2\left.\frac{dt_{\text{SP}}}{d\delta}\right|_{\mathbf{x}_{\text{P}}=\mathbf{x}_{\text{P}}^{\text{min}}} = 0. \tag{7}$$

Because the derivative of $t_{\text{SP}}$ with respect to $\delta$ must be zero when the reflection point is $\mathbf{x}_{\text{P}}^{\text{min}}$, the same must hold for the derivative of $t_{\text{SP}}^2$:

$$\left.\frac{dt_{\text{SP}}^2}{d\delta}\right|_{\mathbf{x}_{\text{P}}=\mathbf{x}_{\text{P}}^{\text{min}}} = 2t_{\text{SP}}\left.\frac{dt_{\text{SP}}}{d\delta}\right|_{\mathbf{x}_{\text{P}}=\mathbf{x}_{\text{P}}^{\text{min}}} = 0, \tag{8}$$

which is easier to compute from (5). In our zero-offset case, $t_{SP}^2$ has the form

$$t_{\text{SP}}^2\big|_{\mathbf{x}_{\text{S}}=\mathbf{x}_{\text{R}}} = \frac{1}{v_1^2}\left[\delta\cos\varphi - L\sin\varphi\right]^2 + \frac{1}{v_2^2}\left[\delta\sin\varphi + L\cos\varphi\right]^2, \tag{9}$$

and its derivative with respect to $\delta$ is

$$\left.\frac{dt_{\text{SP}}^2}{d\delta}\right|_{\mathbf{x}_{\text{S}}=\mathbf{x}_{\text{R}}} = \frac{2\cos\varphi}{v_1^2}\left[\delta\cos\varphi - L\sin\varphi\right] + \frac{2\sin\varphi}{v_2^2}\left[\delta\sin\varphi + L\cos\varphi\right]. \tag{10}$$

By imposing the condition (8), we find that $\delta$ satisfies

$$\delta = \frac{L\sin\varphi\cos\varphi\left[\frac{1}{v_1^2} - \frac{1}{v_2^2}\right]}{\frac{1}{v_1^2}\cos^2\varphi + \frac{1}{v_2^2}\sin^2\varphi} = \frac{L\sin 2\varphi(v_2^2 - v_1^2)}{2(v_1^2\sin^2\varphi + v_2^2\cos^2\varphi)}. \tag{11}$$

Thus, the reflection point of fastest waves propagating from $\mathbf{x}_{\text{S}}$ to $\mathbf{x}_{\text{R}}$ is generally given by

$$\mathbf{x}_{\text{P}}^{\text{min}} = \left(\frac{x_{1,\text{S}} + x_{1,\text{R}}}{2} + \frac{L\sin 2\varphi(v_2^2 - v_1^2)}{2(v_1^2\sin^2\varphi + v_2^2\cos^2\varphi)}, L\right). \tag{12}$$

## IV. Reflector-based experimental setup: first-arrival reflection traveltime

The first-arrival reflection traveltime is the sum of two terms:

$$t_{\text{SR}}(\mathbf{x}_{\text{P}}^{\text{min}}) = t_{\text{SP}}(\mathbf{x}_{\text{P}}^{\text{min}}) + t_{\text{PR}}(\mathbf{x}_{\text{P}}^{\text{min}}). \tag{13}$$

For simplicity, before computing these two traveltimes, we focus on deriving simplified expressions for their squared counterparts:

1) Traveltime from the source to the reflection point:

$$\begin{aligned} t_{\text{SP}}^2\left(\mathbf{x}_{\text{P}}^{\text{min}}\right) = \frac{1}{v_1^2}&\left[\left(\frac{d}{2} + \frac{L\sin 2\varphi(v_2^2 - v_1^2)}{2(v_1^2\sin^2\varphi + v_2^2\cos^2\varphi)}\right)\cos\varphi - L\sin\varphi\right]^2 \\ +\frac{1}{v_2^2}&\left[\left(\frac{d}{2} + \frac{L\sin 2\varphi(v_2^2 - v_1^2)}{2(v_1^2\sin^2\varphi + v_2^2\cos^2\varphi)}\right)\sin\varphi + L\cos\varphi\right]^2, \end{aligned} \tag{14}$$

where $d = x_{1,\text{R}} - x_{1,\text{S}}$ is the source-receiver offset. The terms in brackets can be further simplified as

$$\begin{aligned} \left(\frac{d}{2} + \frac{L\sin 2\varphi(v_2^2 - v_1^2)}{2(v_1^2\sin^2\varphi + v_2^2\cos^2\varphi)}\right)\cos\varphi - L\sin\varphi &= \frac{d}{2}\cos\varphi + L\sin\varphi\left[\frac{\cos^2\varphi(v_2^2 - v_1^2) - (v_1^2\sin^2\varphi + v_2^2\cos^2\varphi)}{v_1^2\sin^2\varphi + v_2^2\cos^2\varphi}\right] \\ &= \frac{d}{2}\cos\varphi - \frac{Lv_1^2\sin\varphi}{v_1^2\sin^2\varphi + v_2^2\cos^2\varphi} \end{aligned} \tag{15}$$

and

$$\left(\frac{d}{2} + \frac{L\sin 2\varphi(v_2^2 - v_1^2)}{2(v_1^2\sin^2\varphi + v_2^2\cos^2\varphi)}\right)\sin\varphi + L\sin\varphi = \frac{d}{2}\sin\varphi + \frac{Lv_2^2\cos\varphi}{v_1^2\sin^2\varphi + v_2^2\cos^2\varphi}. \tag{16}$$

By replacing them in (14), we obtain

$$t_{\text{SP}}^2\left(\mathbf{x}_{\text{P}}^{\text{min}}\right) = \frac{1}{v_1^2}\left[\frac{d}{2}\cos\varphi - \frac{Lv_1^2\sin\varphi}{v_1^2\sin^2\varphi + v_2^2\cos^2\varphi}\right]^2 + \frac{1}{v_2^2}\left[\frac{d}{2}\sin\varphi + \frac{Lv_2^2\cos\varphi}{v_1^2\sin^2\varphi + v_2^2\cos^2\varphi}\right]^2, \tag{17}$$

which reduces to

$$t_{\text{SP}}^2\left(\mathbf{x}_{\text{P}}^{\min}\right) = \frac{d^2}{4v_1^2v_2^2}(v_1^2\sin^2\varphi + v_2^2\cos^2\varphi) + \frac{L^2}{v_1^2\sin^2\varphi + v_2^2\cos^2\varphi} = \frac{d^2}{4v^2(\theta=\pi/2)} + \frac{L^2v^2(\theta=\pi/2)}{v_1^2v_2^2}. \tag{18}$$

We used (1) in the last step.

2) Traveltime from the reflection point to the receiver:

$$\begin{aligned} t_{\text{PR}}^2\left(\mathbf{x}_{\text{P}}^{\min}\right) = \frac{1}{v_1^2}\left[\left(\frac{d}{2} - \frac{L\sin 2\varphi(v_2^2-v_1^2)}{2(v_1^2\sin^2\varphi + v_2^2\cos^2\varphi)}\right)\cos\varphi + L\sin\varphi\right]^2 \\ + \frac{1}{v_2^2}\left[\left(\frac{d}{2} - \frac{L\sin 2\varphi(v_2^2-v_1^2)}{2(v_1^2\sin^2\varphi + v_2^2\cos^2\varphi)}\right)\sin\varphi - L\cos\varphi\right]^2. \end{aligned} \tag{19}$$

Following the same steps as before, we simplify the terms in brackets to obtain

$$t_{\text{PR}}^2\left(\mathbf{x}_{\text{P}}^{\min}\right) = \frac{1}{v_1^2}\left[\frac{d}{2}\cos\varphi + \frac{Lv_1^2\sin\varphi}{v_1^2\sin^2\varphi + v_2^2\cos^2\varphi}\right]^2 + \frac{1}{v_2^2}\left[\frac{d}{2}\sin\varphi - \frac{Lv_2^2\cos\varphi}{v_1^2\sin^2\varphi + v_2^2\cos^2\varphi}\right]^2, \tag{20}$$

which can be further simplified as

$$t_{\text{PR}}^2\left(\mathbf{x}_{\text{P}}^{\min}\right) = \frac{d^2}{4v_1^2v_2^2}(v_1^2\sin^2\varphi + v_2^2\cos^2\varphi) + \frac{L^2}{v_1^2\sin^2\varphi + v_2^2\cos^2\varphi} = \frac{d^2}{4v^2(\theta=\pi/2)} + \frac{L^2v^2(\theta=\pi/2)}{v_1^2v_2^2}. \tag{21}$$

By comparing (21) to (18), we observe that

$$t_{\text{SP}}\left(\mathbf{x}_{\text{P}}^{\min}\right) = t_{\text{PR}}\left(\mathbf{x}_{\text{P}}^{\min}\right), \tag{22}$$

meaning that the fastest ray path is the path with equal traveltime along each segment. Taking this into account, we finally derive the analytical expression for first-arrival reflection traveltime:

$$t_{\text{SR}}^2\left(\mathbf{x}_{\text{P}}^{\min}\right) = 4t_{\text{SP}}^2\left(\mathbf{x}_{\text{P}}^{\min}\right) = \frac{d^2}{v^2(\theta=\pi/2)} + \frac{4L^2v^2(\theta=\pi/2)}{v_1^2v_2^2}. \tag{23}$$

Note that (22) also means that the mirror image of the receiver, namely a virtual receiver $\tilde{R}$ located below the reflector that satisfies $t_{\text{S}\tilde{\text{R}}} = t_{\text{SR}}$, is generally located at

$$\mathbf{x}_{\tilde{\text{R}}} = 2\mathbf{x}_{\text{P}}^{\min} - \mathbf{x}_{\text{S}}. \tag{24}$$

## V. Proof: accuracy of the reflection point

When deriving the reflection point expression, we assumed that this point is shifted from the source-receiver mid-point by the same constant $\delta$ for every source-receiver combination. If this assumption is accurate, the derivative of $t_{\text{SR}}^2(\mathbf{x}_{\text{P}})$ with respect to $\mathbf{x}_{\text{P}}$ (or $x_{1,\text{P}}$ since the reflection point is always at the reflector) will always be zero at $\mathbf{x}_{\text{P}}^{\min}$ given by (12), i.e.,

$$\left.\frac{dt_{\text{SR}}}{dx_{1,\text{P}}}\right|_{\mathbf{x}_{\text{P}}=\mathbf{x}_{\text{P}}^{\min}} = \left.\frac{dt_{\text{SP}}}{dx_{1,\text{P}}}\right|_{\mathbf{x}_{\text{P}}=\mathbf{x}_{\text{P}}^{\min}} + \left.\frac{dt_{\text{PR}}}{dx_{1,\text{P}}}\right|_{\mathbf{x}_{\text{P}}=\mathbf{x}_{\text{P}}^{\min}} = 0. \tag{25}$$

That is, Fermat's principle must be satisfied for any source-receiver combination. In the following, we prove that (25) always holds for $\mathbf{x}_{\text{P}}^{\min}$ given by (12).

As before, we transform the derivatives in (25) using squared traveltimes as

$$\left.\frac{dt_{\text{SR}}}{dx_{1,\text{P}}}\right|_{\mathbf{x}_{\text{P}}=\mathbf{x}_{\text{P}}^{\min}} = \left.\left[\frac{1}{2t_{\text{SP}}}\frac{dt_{\text{SP}}^2}{dx_{1,\text{P}}} + \frac{1}{2t_{\text{PR}}}\frac{dt_{\text{PR}}^2}{dx_{1,\text{P}}}\right]\right|_{\mathbf{x}_{\text{P}}=\mathbf{x}_{\text{P}}^{\min}} = \frac{1}{2t_{\text{SP}}(\mathbf{x}_{\text{P}}^{\min})}\left.\left[\frac{dt_{\text{SP}}^2}{dx_{1,\text{P}}} + \frac{dt_{\text{PR}}^2}{dx_{1,\text{P}}}\right]\right|_{\mathbf{x}_{\text{P}}=\mathbf{x}_{\text{P}}^{\min}} = 0. \tag{26}$$

The last step uses the equality given in (22). Therefore, this equation is satisfied when

$$\left.\frac{dt_{\text{SP}}^2}{dx_{1,\text{P}}}\right|_{\mathbf{x}_{\text{P}}=\mathbf{x}_{\text{P}}^{\min}} = -\left.\frac{dt_{\text{PR}}^2}{dx_{1,\text{P}}}\right|_{\mathbf{x}_{\text{P}}=\mathbf{x}_{\text{P}}^{\min}}. \tag{27}$$

To see if this is true, we compute both derivatives:

1) Derivative of $t_{\text{SP}}^2$ at $\mathbf{x}_{\text{P}}^{\min}$:

$$\left.\frac{dt_{\text{SP}}^2}{dx_{1,\text{P}}}\right|_{\mathbf{x}_{\text{P}}=\mathbf{x}_{\text{P}}^{\min}} = \frac{2\cos\varphi}{v_1^2}\left[(x_{1,\text{P}} - x_{1,\text{S}})\cos\varphi - L\sin\varphi\right] + \frac{2\sin\varphi}{v_2^2}\left[(x_{1,\text{P}} - x_{1,\text{S}})\sin\varphi + L\cos\varphi\right]\Big|_{\mathbf{x}_{\text{P}}=\mathbf{x}_{\text{P}}^{\min}}. \tag{28}$$

Here, we can use (17) to simplify the terms in brackets after evaluating them at $\mathbf{x}_{\text{P}}^{\min}$:

$$\left.\frac{dt_{\text{SP}}^2}{dx_{1,\text{P}}}\right|_{\mathbf{x}_{\text{P}}=\mathbf{x}_{\text{P}}^{\min}} = \frac{2\cos\varphi}{v_1^2}\left[\frac{d}{2}\cos\varphi - \frac{Lv_1^2\sin\varphi}{v_1^2\sin^2\varphi + v_2^2\cos^2\varphi}\right] + \frac{2\sin\varphi}{v_2^2}\left[\frac{d}{2}\sin\varphi + \frac{Lv_2^2\cos\varphi}{v_1^2\sin^2\varphi + v_2^2\cos^2\varphi}\right], \tag{29}$$

which can be further simplified as

$$\left.\frac{dt_{\text{SP}}^2}{dx_{1,\text{P}}}\right|_{\mathbf{x}_\text{P}=\mathbf{x}_\text{P}^{\min}} = d\left(\frac{\cos^2\varphi}{v_1^2}+\frac{\sin^2\varphi}{v_2^2}\right). \tag{30}$$

2) Derivative of $t_{\text{PR}}^2$ at $\mathbf{x}_\text{P}^{\min}$:

$$\left.\frac{dt_{\text{PR}}^2}{dx_{1,\text{P}}}\right|_{\mathbf{x}_\text{P}=\mathbf{x}_\text{P}^{\min}} = \frac{-2\cos\varphi}{v_1^2}\left[(x_{1,\text{R}}-x_{1,\text{P}})\cos\varphi + L\sin\varphi\right] - \frac{2\sin\varphi}{v_2^2}\left[(x_{1,\text{R}}-x_{1,\text{P}})\sin\varphi - L\cos\varphi\right]\Bigg|_{\mathbf{x}_\text{P}=\mathbf{x}_\text{P}^{\min}}. \tag{31}$$

As before, we can use (20) to simplify the terms in brackets after evaluating them at $\mathbf{x}_\text{P}^{\min}$:

$$\left.\frac{dt_{\text{PR}}^2}{dx_{1,\text{P}}}\right|_{\mathbf{x}_\text{P}=\mathbf{x}_\text{P}^{\min}} = \frac{-2\cos\varphi}{v_1^2}\left[\frac{d}{2}\cos\varphi + \frac{Lv_1^2\sin\varphi}{v_1^2\sin^2\varphi+v_2^2\cos^2\varphi}\right] - \frac{2\sin\varphi}{v_2^2}\left[\frac{d}{2}\sin\varphi - \frac{Lv_2^2\cos\varphi}{v_1^2\sin^2\varphi+v_2^2\cos^2\varphi}\right], \tag{32}$$

which can be further simplified as

$$\left.\frac{dt_{\text{PR}}^2}{dx_{1,\text{P}}}\right|_{\mathbf{x}_\text{P}=\mathbf{x}_\text{P}^{\min}} = -d\left(\frac{\cos^2\varphi}{v_1^2}+\frac{\sin^2\varphi}{v_2^2}\right). \tag{33}$$

By comparing (30) and (33), we see that (27) is satisfied, meaning that the expression of the reflection point given in (12) is exact and does not involve any approximation.

## VI. Reflector inclination: derivation of the reflection point

In this subsection, we calculate the reflection point for an experimental setup with an inclined reflector. To take advantage of our previous results, we use the equivalent experimental setup depicted in Fig. 1 and consider a virtual source $\tilde{S}$ with the same elevation as the receiver $R$. The horizontal distance between $\tilde{S}$ and the reflection point $P$ is then given by

$$\tilde{x}_{1,\text{P}} = x_{1,\text{P}} + x = \frac{d\cos\alpha + x}{2} + \delta', \tag{34}$$

where

$$\delta' = \frac{(L + d\sin\alpha)\sin 2\varphi(v_2^2 - v_1^2)}{2(v_1^2\sin^2\varphi + v_2^2\cos^2\varphi)}. \tag{35}$$

The last step uses our previous result in (12). From here, we see that the horizontal distance between the actual source $S$ and the reflection point $P$ is

$$x_{1,\text{P}} = \frac{d\cos\alpha - x}{2} + \delta'. \tag{36}$$

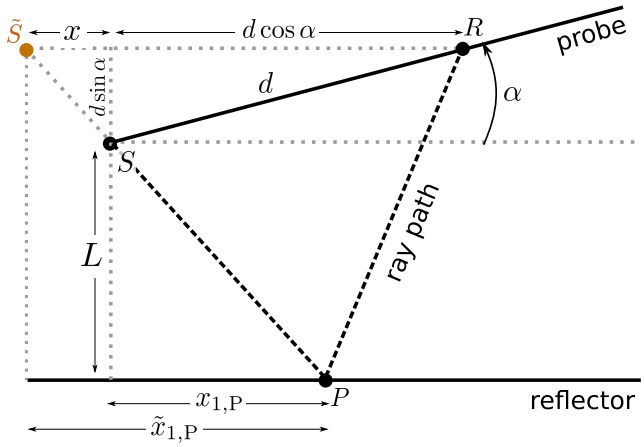


Fig. 1. Schematic illustration of the experimental setup with an inclined ultrasound probe by $\alpha$ and a horizontal reflector in front of it. This setup is equivalent to having an inclined reflector in front of a horizontally placed linear probe [see Fig. 3 in the main manuscript]. The vertical probe-reflector distance $L$ is measured from the first transducer element, where in this example we locate the source $S$. $R$ denotes the receiver located at a distance $d$ from $S$, $P$ is the reflection point, and $\tilde{S}$ is a virtual source with same elevation as $R$. The horizontal distance between $\tilde{S}$ and $S$ is $x$. This virtual source will allow us to compute the reflection point using (12).

We can find a second relationship between $x$ and $x_{1,\text{P}}$ using the trigonometric identity

$$\frac{d\sin\alpha}{x} = \frac{L}{x_{1,\text{P}}} \quad \Rightarrow \quad x = \frac{x_{1,\text{P}}d\sin\alpha}{L}. \tag{37}$$

Finally, upon inserting (37) in (36), we obtain

$$x_{1,\mathrm{P}} = \frac{d\cos\alpha}{2} - \frac{x_{1,\mathrm{P}}\sin\alpha}{2L} + \delta' \quad \Rightarrow \quad x_{1,\mathrm{P}} = \frac{L(d\cos\alpha + 2\delta')}{2L + d\sin\alpha}. \tag{38}$$

We can generalize this expression by dropping the assumption that $S$ is located at the origin of the coordinate system. Then, the reflection point becomes

$$x_{1,\mathrm{P}} = d_{\mathrm{S}}\cos\alpha + \frac{(L + d_{\mathrm{S}}\sin\alpha)(d\cos\alpha + 2\delta')}{2(L + d_{\mathrm{S}}\sin\alpha) + d\sin\alpha}, \tag{39}$$

with

$$\delta' = \frac{(L + d_{\mathrm{S}}\sin\alpha + d\sin\alpha)\sin 2\varphi(v_2^2 - v_1^2)}{2(v_1^2\sin^2\varphi + v_2^2\cos^2\varphi)}, \tag{40}$$

where $d_{\mathrm{S}}$ is the distance between the source and the origin of the coordinate system (i.e., the first transducer element of the probe).

## VII. Reflector inclination: first-arrival reflection traveltime

For simplicity, we calculate the traveltime $t_{\mathrm{SR}}$ considering the mirror image of the receiver $\tilde{R}$. This virtual receiver is located below the reflector, where $t_{\mathrm{S\tilde{R}}} = t_{\mathrm{SR}}$ is satisfied. When the reflector is not inclined, the location of the virtual receiver is given by (24). In our example, therefore, this location is $\mathbf{x}_{\tilde{\mathrm{R}}} = (2\tilde{x}_{1,\mathrm{P}} - x, 2L + d\sin\alpha) = (d\cos\alpha + 2\delta', 2L + d\sin\alpha)$, shown in Fig. 2. Note that we again place the origin of the coordinate system at $S$.

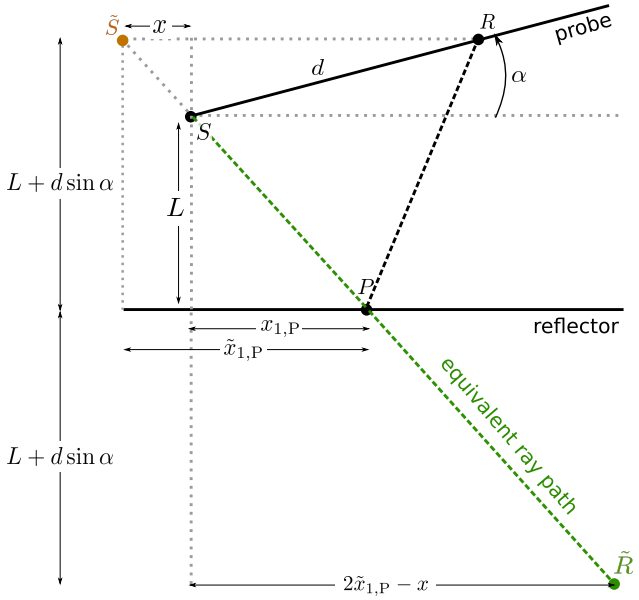


Fig. 2. Schematic illustration showing the location of the mirror image $\tilde{R}$ of the receiver $R$. The traveltime of a straight ray traveling from $S$ to $\tilde{R}$ (green dashed line) is the same as the first-arrival reflection traveltime from $S$ to $R$, that is, $t_{\mathrm{S\tilde{R}}} = t_{\mathrm{SR}}$. This virtual receiver is located at $\mathbf{x}_{\tilde{\mathrm{R}}} = (2\tilde{x}_{1,\mathrm{P}} - x, 2L + d\sin\alpha)$ with the origin of the coordinate system at $S$. We refer the reader to Fig. 1 to understand the meaning of the rest of the symbols in the image.

Following (5), the traveltime between $S$ and $\tilde{R}$ is given by

$$t_{\mathrm{S\tilde{R}}}^2 = \frac{1}{v_1^2}\underbrace{\left[(d\cos\alpha + 2\delta')\cos\varphi - (2L + d\sin\alpha)\sin\varphi\right]^2}_{\mathrm{I}^2} + \frac{1}{v_2^2}\underbrace{\left[(d\cos\alpha + 2\delta')\sin\varphi + (2L + d\sin\alpha)\cos\varphi\right]^2}_{\mathrm{II}^2}. \tag{41}$$

To simplify this expression, we first simplify the terms in brackets separately using the definition of $\delta'$ in (35):

1) The first term can be reduced to

$$\mathrm{I} = d\cos(\varphi + \alpha) + \frac{d\sin\alpha\sin 2\varphi\cos\varphi(v_2^2 - v_1^2) - 2Lv_1^2\sin\varphi}{v_1^2\sin^2\varphi + v_2^2\cos^2\varphi}. \tag{42}$$

After taking the square of this term and dividing it with $v_1^2$, we obtain

$$\begin{aligned}\frac{\mathrm{I}^2}{v_1^2} = \frac{d^2\cos^2(\varphi+\alpha)}{v_1^2} + 4d\sin\varphi\cos(\varphi+\alpha)\frac{\left(d\sin\alpha\cos^2\varphi\left(\frac{v_2^2-v_1^2}{v_1^2}\right) - L\right)}{v_1^2\sin^2\varphi + v_2^2\cos^2\varphi} \\ + \frac{d^2\sin^2\alpha\sin^2 2\varphi\cos^2\varphi\left(\frac{v_2^2-v_1^2}{v_1}\right)^2 - 2Ld\sin\alpha\sin^2 2\varphi(v_2^2 - v_1^2) + 4L^2v_1^2\sin^2\varphi}{(v_1^2\sin^2\varphi + v_2^2\cos^2\varphi)^2}.\end{aligned} \tag{43}$$

2) The second term can be reduced to

$$\mathrm{II} = d\sin(\varphi+\alpha) + \frac{d\sin\alpha\sin 2\varphi\sin\varphi(v_2^2-v_1^2)+2Lv_2^2\cos\varphi}{v_1^2\sin^2\varphi+v_2^2\cos^2\varphi}. \tag{44}$$

As before, we take the square of II and divide it with $v_2^2$ to obtain

$$\begin{aligned}\frac{\mathrm{II}^2}{v_2^2} = \frac{d^2\sin^2(\varphi+\alpha)}{v_2^2} &+ 4d\cos\varphi\sin(\varphi+\alpha)\frac{\left(d\sin\alpha\sin^2\varphi\left(\frac{v_2^2-v_1^2}{v_2^2}\right)+L\right)}{v_1^2\sin^2\varphi+v_2^2\cos^2\varphi}\\ &+\frac{d^2\sin^2\alpha\sin^2 2\varphi\sin^2\varphi\left(\frac{v_2^2-v_1^2}{v_2}\right)^2+2Ld\sin\alpha\sin^2 2\varphi(v_2^2-v_1^2)+4L^2v_2^2\cos^2\varphi}{(v_1^2\sin^2\varphi+v_2^2\cos^2\varphi)^2}.\end{aligned} \tag{45}$$

We notice that (43) and (45) have common terms that will vanish when we sum them to calculate $t_{\mathrm{S\tilde{R}}}^2$. Moreover, using the symmetries between their terms, we can express the traveltime as

$$\begin{aligned}t_{\mathrm{S\tilde{R}}}^2 = \; & d^2\left(\frac{\sin^2(\varphi+\alpha)}{v_2^2}+\frac{\cos^2(\varphi+\alpha)}{v_1^2}\right)\\ &+\frac{4Ld\sin\alpha-d^2\sin^2\alpha\sin^2 2\varphi\frac{(v_1^2-v_2^2)^2}{v_1^2v_2^2}}{v_1^2\sin^2\varphi+v_2^2\cos^2\varphi}+d^2\sin 2\alpha\sin 2\varphi\frac{v_2^2-v_1^2}{v_1^2v_2^2}\\ &+\frac{4L^2+d^2\sin^2\alpha\sin^2 2\varphi\frac{(v_2^2-v_1^2)^2}{v_1^2v_2^2}}{v_1^2\sin^2\varphi+v_2^2\cos^2\varphi},\end{aligned} \tag{46}$$

where each line in this equation refers to one term in (43) and (45), following the same order. We can futher simplify (46) as

$$\begin{aligned}t_{\mathrm{S\tilde{R}}}^2 = \; & d^2\left(\frac{\sin^2(\varphi+\alpha)}{v_2^2}+\frac{\cos^2(\varphi+\alpha)}{v_1^2}\right)\\ &+\frac{4L(L+d\sin\alpha)}{v_1^2\sin^2\varphi+v_2^2\cos^2\varphi}+d^2\sin 2\alpha\sin 2\varphi\frac{v_2^2-v_1^2}{v_1^2v_2^2}.\end{aligned} \tag{47}$$

Here, the sum of the first and third term equals to

$$d^2\left(\frac{\sin^2(\varphi+\alpha)}{v_2^2}+\frac{\cos^2(\varphi+\alpha)}{v_1^2}\right)+d^2\sin 2\alpha\sin 2\varphi\frac{v_2^2-v_1^2}{v_1^2v_2^2} = \frac{d^2}{v_1^2v_2^2}\left(v_1^2\sin^2(\varphi-\alpha)+v_2^2\cos^2(\varphi-\alpha)\right). \tag{48}$$

Therefore, the traveltime $t_{\mathrm{S\tilde{R}}}^2$, which is equal to $t_{\mathrm{SR}}^2$, reduces to

$$t_{\mathrm{SR}}^2 = \frac{d^2}{v_1^2v_2^2}\left(v_1^2\sin^2(\varphi-\alpha)+v_2^2\cos^2(\varphi-\alpha)\right)+\frac{4L(L+d\sin\alpha)}{v_1^2\sin^2\varphi+v_2^2\cos^2\varphi}. \tag{49}$$

So far, we have considered the experimental setup depicted in Figs. 1 and 2. However, this setup is a rotated version of the actual experimental configuration considered in the main manuscript, as shown in Fig. 3. To find an expression for the traveltime that is valid for our original experimental setup, we need to apply the transformations $L \to L\cos\alpha$ and $\varphi \to \varphi+\alpha$. The transformation for $L$ considers the case in which the source is located at the first transducer element (origin of the coordinate system). We can generalize the traveltimes to any source location applying the transformation $L \to L\cos\alpha + d_{\mathrm{S}}\sin\alpha$, where $d_{\mathrm{S}}$ is the distance between $S$ and the origin of the coordinate system. Thus, the first-arrival reflection traveltime between $S$ and $R$ becomes

$$t_{\mathrm{SR}}^2 = \frac{d^2}{v^2(\pi/2)}+\frac{4L'(L'+d\sin\alpha)}{v_1^2\sin^2(\varphi+\alpha)+v_2^2\cos^2(\varphi+\alpha)} \tag{50}$$

with

$$L' = L\cos\alpha + d_{\mathrm{S}}\sin\alpha. \tag{51}$$

## VIII. Constraining anisotropy parameters

In this section, we show additional figures to clarify the content of Fig. 4 in the main manuscript. This figure represents the equivalent models in terms of the anisotropy angle and the velocity ratio. This is useful to visualize three-dimensional models in a two-dimensional image. However, it may not be clear whether each point in this figure corresponds to a single anisotropy model or a set of models with equal velocity ratio. In order to clarify this point, we show two additional figures of the same result. Figure 4(a) shows the parameters $\varphi$ and $v_1$ of the models, whereas Figure 4(b) shows $\varphi$ and $v_1$. We can see that each point in Fig. 4 of the main manuscript and the intersection point of the curves represent a single anisotropy model.

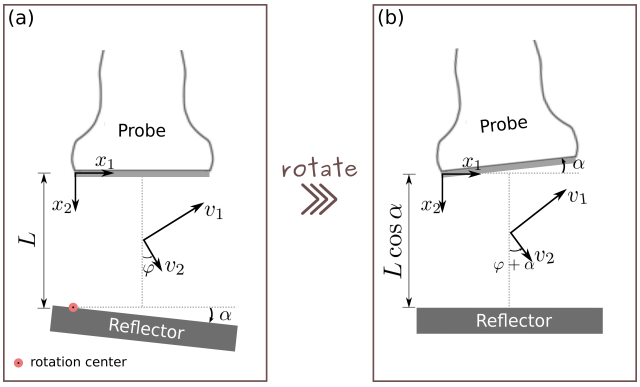


Fig. 3. Schematic illustration showing two equivalent experimental setups. (a) Our original setup considers the reflector inclined by $\alpha$ with respect to the $x_1$-axis. The vertical distance between the first transducer element (origin of the coordinate system) and the reflector is $L$. The anisotropy symmetry axis of the medium has the orientation $\varphi$ with respect to the $x_2$-axis. (b) We rotate the whole system by $\alpha$ in order to imagine an equivalent setup with no reflector inclination. Now, the probe is inclined with respect to the $x_1$-axis, the anisotropy of the medium has the orientation $\varphi + \alpha$, and the vertical probe-reflector distance becomes $L\cos\alpha$.

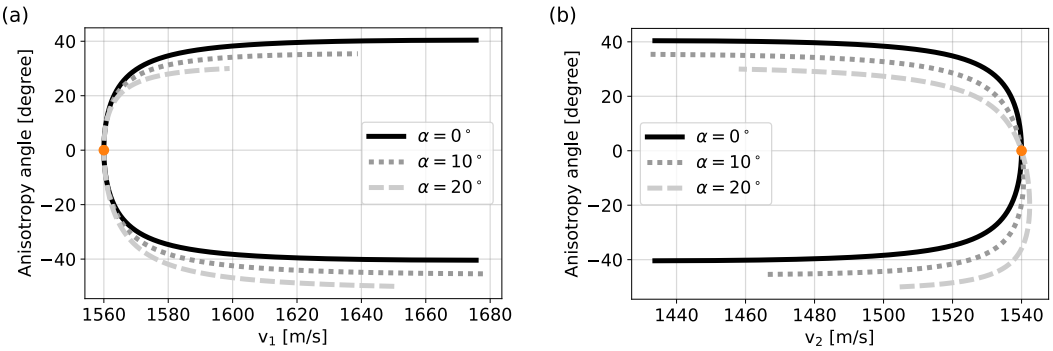


Fig. 4. Figures corresponding to the result shown in Fig. 4 of the main manuscript. We show muscle models equivalent to $\hat{\mathbf{m}} = (1560\text{ m/s}, 1540\text{ m/s}, 0°)$ (orange) in terms of first-arrival reflection traveltimes using reflector inclination angles $\alpha = 0°, 10°$, and $20°$. Each model is defined by three parameters: anisotropy angle $\varphi$ and velocities $v_1$ and $v_2$. For visualization, we show in (a) the parameters $\varphi$ and $v_1$ of the models and in (b) the parameters $\varphi$ and $v_2$ of the same models. We can observe that the three curves intersect in a single point that represents $\hat{\mathbf{m}}$.

## IX. Extended Bayesian formulation for uncertain reflector inclination angles

In this section, we show numerical examples supporting the uniqueness of the solution shown in Fig. 9(b) (in gray) of the main manuscript. We use the same Bayesian formulation that considers inclination angles as unknown model parameters and perform the inversion initializing the Metropolis-Hastings Markov chain Monte Carlo (MCMC) algorithm with models that deviate strongly from the true model $\mathbf{m}_{\text{true}} = (1560\text{ m/s}, 1540\text{ m/s}, 0°, 0°, 5°)$. This allows us to explore a wider area of the model space and converge to other maxima of the posterior probability density function, if any. Figs. 5–7 show the results obtained when the MCMC is initialized with models $\mathbf{m}_{\text{init}} = (1350\text{ m/s}, 1350\text{ m/s}, 40°, 10°, 15°)$, $\mathbf{m}_{\text{init}} = (1750\text{ m/s}, 1750\text{ m/s}, -40°, 15°, 15°)$, $\mathbf{m}_{\text{init}} = (1750\text{ m/s}, 1750\text{ m/s}, 40°, 15°, 0°)$, $\mathbf{m}_{\text{init}} = (1310\text{ m/s}, 1310\text{ m/s}, -40°, 15°, 0°)$, $\mathbf{m}_{\text{init}} = (1310\text{ m/s}, 1750\text{ m/s}, 40°, 5°, 0°)$, and $\mathbf{m}_{\text{init}} = (1750\text{ m/s}, 1310\text{ m/s}, -40°, 5°, 0°)$. Note that parameter values chosen for these initial models are close to the extreme limits imposed by our uniform priors, which are defined within the range of $[1300\text{ m/s}, 1800\text{ m/s}]$ and $[-45°, 45°)$ for velocities and the anisotropy angle, respectively. Yet, all MCMC realizations converge to the same maximum of the posterior as in Fig. 9(b) (gray), suggesting that the solution uniqueness is still given within the model subspace defined by the priors in this extended Bayesian formulation.

## X. Phase velocities in elliptically anisotropic media

The Christoffel equation relates the stiffness tensor $c_{ijkl}$ to the phase velocities $V$ as

$$\det[c_{ijkl}n_i n_l - \rho V^2 \delta_{jk}] = 0, \tag{52}$$

where the Einstein summation convention is implied for repeated indices. Here, $\rho$ denotes medium density, $\delta_{jk}$ is the Kronecker delta, and $n_i$ refers to the $i$th component of the wavefront normal vector. If we assume the muscle as an elliptically anisotropic medium, the stiffness tensor will have only three relevant components, which are $c_{1111} \equiv c_{11}$, $c_{1122} \equiv c_{12}$, and $c_{2222} \equiv c_{22}$ in Voigt notation.

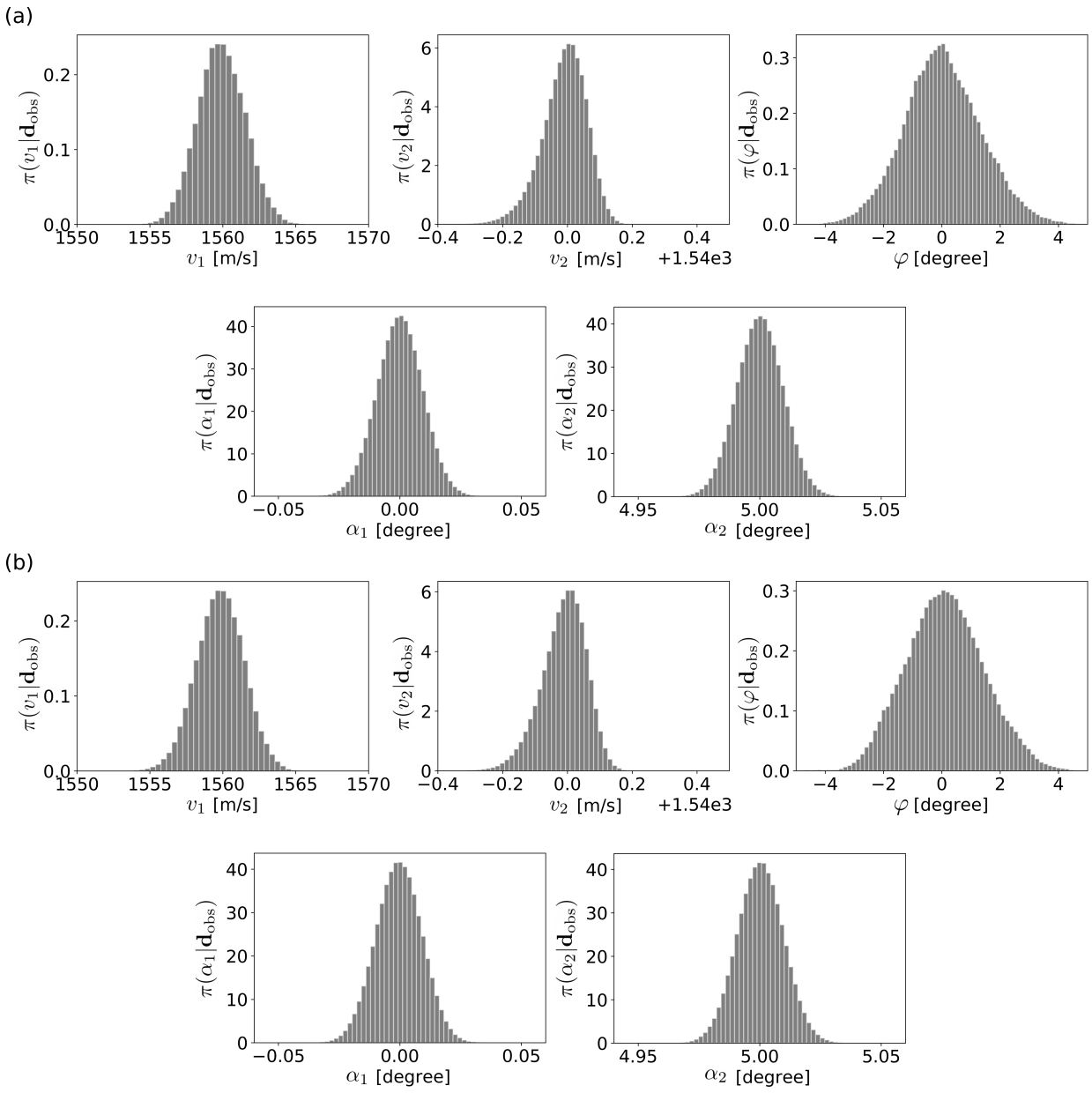


Fig. 5. Marginal probability density functions obtained when we initialize the Metropolis-Hastings Markov chain Monte Carlo algorithm with models (a) $\mathbf{m}_{\rm init} = (1350 \text{ m/s}, 1350 \text{ m/s}, 40°, 10°, 15°)$ and (b) $\mathbf{m}_{\rm init} = (1750 \text{ m/s}, 1750 \text{ m/s}, -40°, 15°, 15°)$.

We consider a two-dimensional problem defined in the $x_1x_2$-plane. For an arbitrary wavefront direction $\mathbf{n} = (\sin\phi, \cos\phi)$, the determinant in (52) reduces to

$$\begin{vmatrix} c_{11}\sin^2\phi - \rho V^2 & c_{12}\sin\phi\cos\phi \\ c_{12}\sin\phi\cos\phi & c_{22}\cos^2\phi - \rho V^2 \end{vmatrix} = \rho^2 V^4 - \rho V^2(c_{11}\sin^2\phi + c_{22}\cos^2\phi) + (c_{11}c_{22} - c_{12}^2)\sin^2\phi\cos^2\phi. \tag{53}$$

Following (52), we equate (53) to zero. This gives a second order polynomial for $\rho V^2$ with solutions

$$\rho V^2 = \frac{1}{2}\left[(c_{11}\sin^2\phi + c_{22}\cos^2\phi) \pm \sqrt{(c_{11}\sin^2\phi + c_{22}\cos^2\phi)^2 - 4(c_{11}c_{22} - c_{12}^2)\sin^2\phi\cos^2\phi}\right]. \tag{54}$$

Here we can simplify the term inside the square root as

$$\rho V^2 = \frac{1}{2}\left[(c_{11}\sin^2\phi + c_{22}\cos^2\phi) \pm \sqrt{(c_{11}\sin^2\phi - c_{22}\cos^2\phi)^2 + c_{12}^2\sin^2 2\phi}\right]. \tag{55}$$

In general, only the positive sign guarantees a solution for $V$. Thus, the phase velocity of longitudinal waves is given by

$$V^2(\phi) = \frac{1}{2\rho}\left[c_{11}\sin^2\phi + c_{22}\cos^2\phi + G(\phi)\right] \tag{56}$$

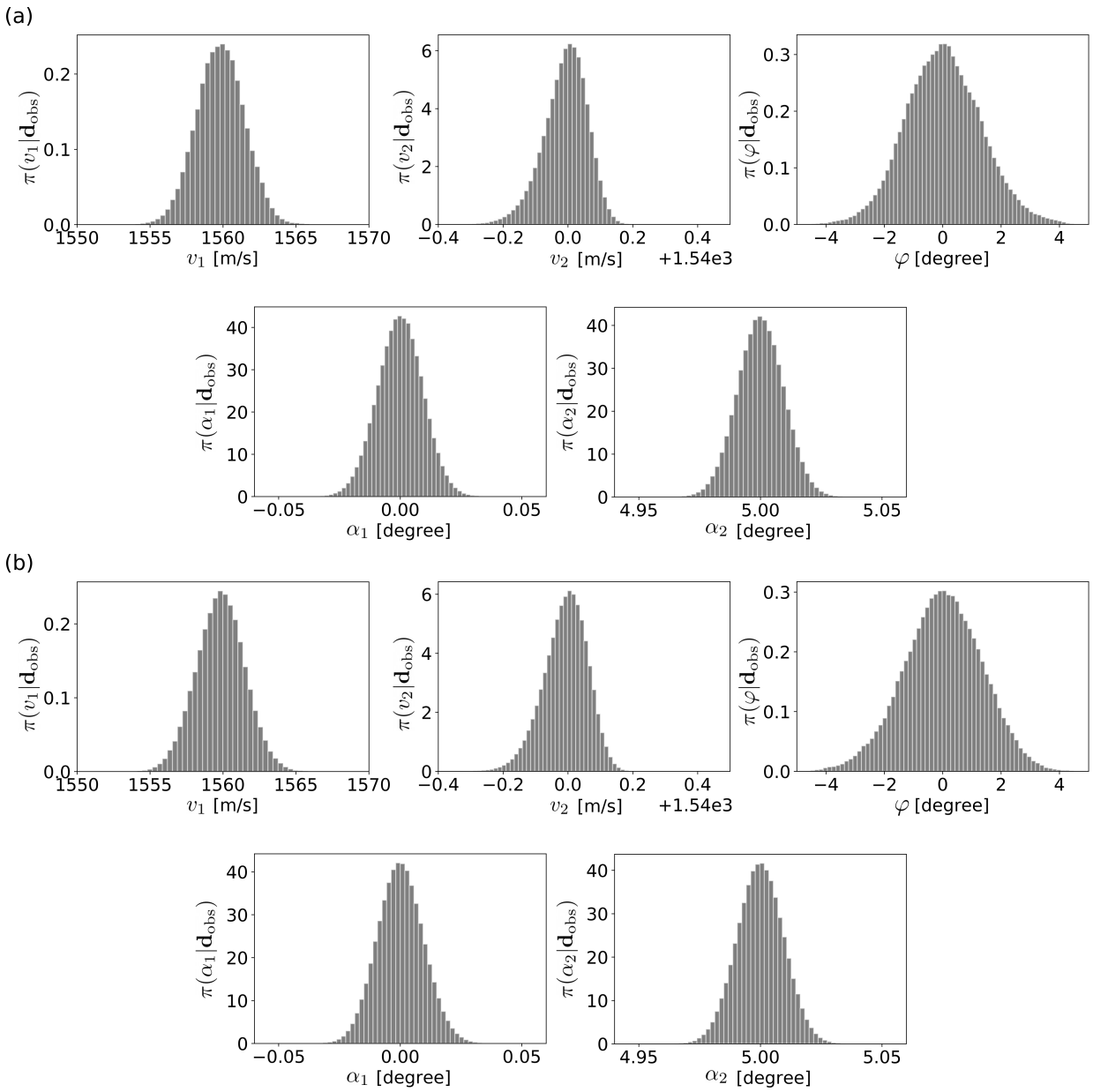


Fig. 6. Marginal probability density functions obtained when we initialize the Metropolis-Hastings Markov chain Monte Carlo algorithm with models (a) $\mathbf{m}_{\rm init} = (1750 \text{ m/s}, 1750 \text{ m/s}, 40°, 15°, 0°)$ and (b) $\mathbf{m}_{\rm init} = (1310 \text{ m/s}, 1310 \text{ m/s}, -40°, 15°, 0°)$.

with

$$G(\phi) = \left[ \left( c_{11} \sin^2 \phi - c_{22} \cos^2 \phi \right)^2 + c_{12}^2 \sin^2 2\phi \right]^{\frac{1}{2}} . \tag{57}$$

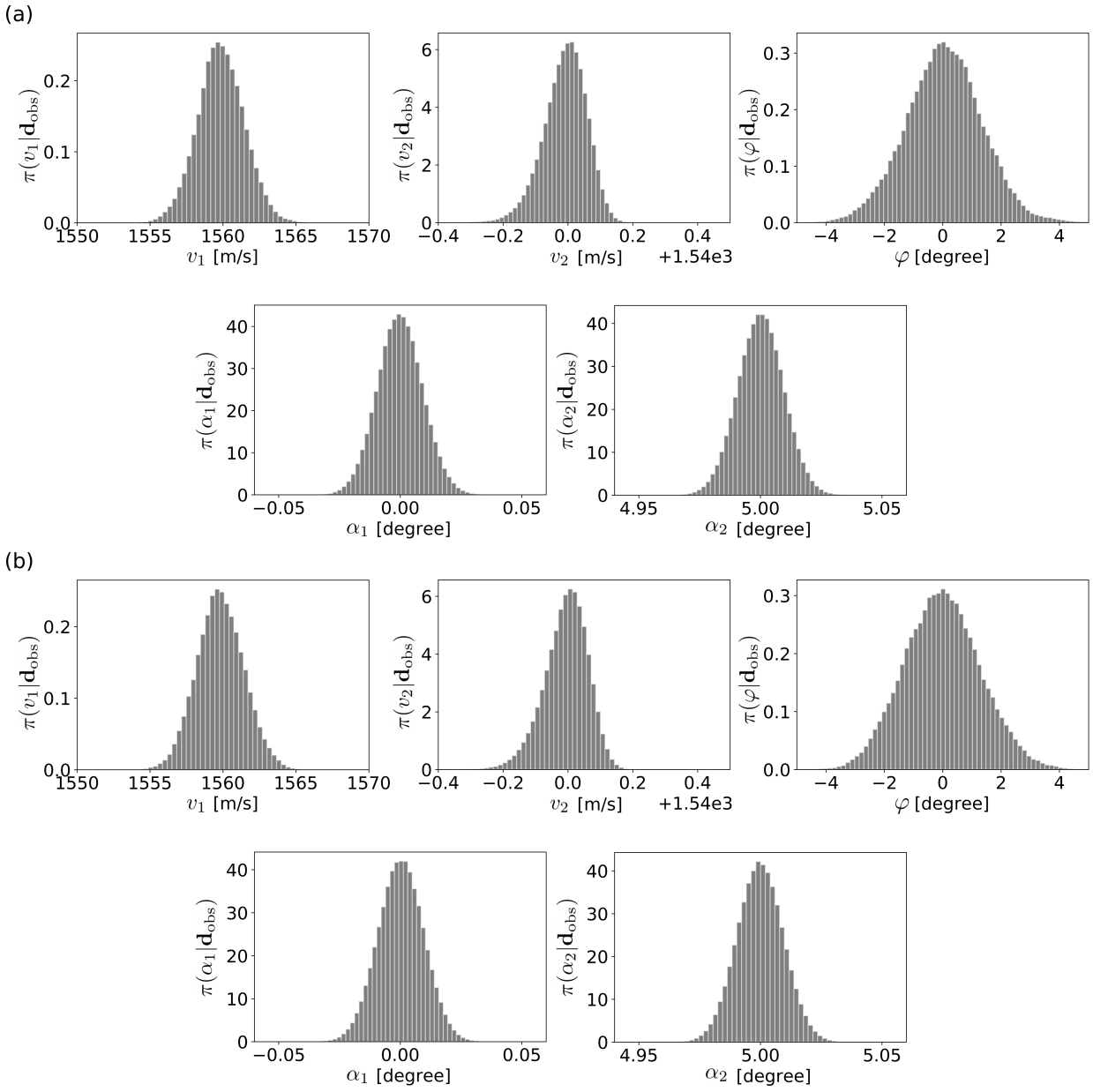


Fig. 7. Marginal probability density functions obtained when we initialize the Metropolis-Hastings Markov chain Monte Carlo algorithm with models (a) $\mathbf{m}_{\rm init} = (1310 \text{ m/s}, 1750 \text{ m/s}, 40^\circ, 5^\circ, 0^\circ)$ and (b) $\mathbf{m}_{\rm init} = (1750 \text{ m/s}, 1310 \text{ m/s}, -40^\circ, 5^\circ, 0^\circ)$.